Fault Diagnosis for Robot Manipulators via Vision Servoing Based Suboptimal Second Order Sliding Mode

Gian Paolo Incremona[1] and Antonella Ferrara[2]

Abstract— **This paper deals with the formulation of a fault diagnosis strategy for industrial robotic manipulators. The core of the proposed scheme is the inverse dynamics-based feedback linearized robotic MIMO system, that is a set of linearized decoupled SISO systems affected by uncertain terms. Relying on this set of systems, in the paper the problem of detecting and isolating both sensor and actuator faults is considered. The proposed fault diagnosis strategy consists of a vision based logic, to detect possible malfunctions of the sensors of the robot, and a set of Unknown Input Observers (UIOs) of second order sliding mode type, to perform the Fault Detection and Isolation (FDI) on the actuators. The sliding mode approach provides good performance in terms of stability and robustness, while guaranteeing a satisfactory estimate of the faults. To give the possibility to the fault diagnosis system to distinguish between sensor and actuator faults, a vision sensor is used in the scheme. This sensor also allows to design a fault tolerant control strategy in case of sensor faults. The verification and the validation of the present proposal have been carried out, both in simulation and experimentally, on an industrial robotic manipulator.**

I. Introduction

In the last decades, there has been a growing interest in methods to detect the occurrence of faults/corruptions in mechanical or electromechanical systems (see, for instance, [1], [2]), and to perform a complete diagnosis of the faulty system. Fault diagnosis, apart from the "detection", which is the capability to reveal the presence of a fault in the system, consists of the so-called "isolation" (the possibility to isolate the faulty component), and of fault "identification", i.e., the reconstruction of the time evolution of the detected fault. The design of an efficient and reliable fault diagnosis strategy can significantly reduce the damage risk, decreasing, as a consequence, the system maintenance costs, while increasing industrial production throughput and operation security [3].

In the scientific literature, the fault diagnosis problem has been faced from a theoretical viewpoint. It has been widely investigated in case of linear, nonlinear and coupled systems. The proposed methods can be classified in "active" or "passive" techniques. The active approach is based on the injection of signals into the system to improve the detectability of the faults (see, among others, [4]–[6]), that is to make abnormal behaviors, which otherwise could remain undetected, more evident. The passive approach is instead based on the comparison between the actual process input-output measurements and the corresponding signals produced, under the assumption of fault absence, by a nominal model of the process, or available under the form of historical data [3], [7].

In most cases, in fault diagnosis literature, the coupling effects in the system are considered negligible, which is generally false in robotics. For this reason, robot fault diagnosis is a particularly difficult problem [8], [9]. In case of robotic systems, the considered faults typically affect the robot actuators and sensors. In field implementations, faults can occur simultaneously on both types of devices. Moreover, more than one fault at a time can perturb the system operations. Yet, in most papers published up to now about fault diagnosis in the robotic context, the assumption that the faults (often assumed to be single faults) affect only the actuators or only the sensors is normally introduced [10]–[13]. Indeed, the difficulty in isolating the faults is due to the relevant coupling effects among the robot joints. This latter can make the occurrence of a fault on an actuator indistinguishable from that of a fault on a sensor, and vice versa.

A preliminary attempt to extend the capability of a fault diagnosis system for robot manipulators to more complex (and realistic) fault scenarios has been made in [14]. The key idea, in that paper, was the use of vision. Yet, the fault diagnosis was still complicated by the nonlinear couplings among the different degrees of mobility of the robot arm. In the present paper, we have elaborated the idea and made it effective by first solving the problem of the rejection of the coupling effects, by relying on an inverse dynamics control approach [15]. The internal control loop transforms the MIMO nonlinear and coupled robotic system into a set of linear decoupled systems affected by bounded uncertainty terms to account for the non idealities in the feedback linearization. The use of a low cost vision sensor (an IP camera in our case) allows one to detect possible sensor faults. In case a sensor fault is revealed, then the joint variables measurements, determined through an appropriate image processing and the application of the inverse kinematics of the robot, are used to close the control feedback, enriching the scheme with a sensor fault tolerant control feature. As for the actuator faults, a number of unknown input observers equal to the number of actuators are exploited to perform the complete fault diagnosis. In this paper, to comply with robustness and smoothness requirements, the second order sliding mode methodology has been adopted to design such observers [16]. More specifically, observer input laws of Suboptimal Second

This is the final version of the accepted paper submitted for inclusion in the Proceedings of the European Control Conference 2019, Naples, Italy, Jun. 2019. [1]G. P. Incremona is with Dipartimento di Elettronica, Informazione e Bioingegneria, Politecnico di Milano, Piazza Leonardo da Vinci 32, 20133, Milano, Italy (gianpaolo.incremona@polimi.it)

[2]A. Ferrara is with Dipartimento di Ingegneria Industriale e dell'Informazione, University of Pavia, Via Ferrata 5, 27100, Pavia, Italy (antonella.ferrara@unipv.it)

Order Sliding Mode (SSOSM) type [17] have been proposed. Note that sliding mode and SSOSM approaches have already been efficiently applied to solve motion and force control problem in case of industrial robots [18]–[21].

Moreover, it is worth recalling that the use of sliding mode theory to solve observation and fault detection problems has already been investigated in the literature (see for instance, [22]–[24], and the references therein cited), even in case of robotic systems (e.g., [13], [25]). Yet, this paper differs from previous proposals because of the joint use of the inverse dynamics approach, of vision and of a battery of SSOSM unknown input observers, which actually enables to solve the fault diagnosis problem for robot manipulators even in case of multiple faults occurring, at the same time, on both the robot actuators and sensors. The proposed fault diagnosis scheme has been assessed in simulation, as well as experimentally.

II. Preliminaries on Vision Servoing System

Some preliminary issues about vision based control (see [15, Chapter 10]), also referred as to Vision Servoing System (VSS), for a n-joints robot manipulator are hereafter introduced.

A. Position reconstruction

Define the planes on which the light reflected by the object is focused and where the photosensitive sensor lies as "image planes". The relationship between the homogeneous coordinates of position, $\widetilde{p} = [p_x,\, p_y,\, p_z,\, 1]^\top$, and the corresponding pixel coordinates in the image plane $(X_\mathrm{I}, Y_\mathrm{I})$ can be written as $\lambda[X_\mathrm{I}, Y_\mathrm{I}, 1]^\top = \Omega\Pi\widetilde{p}$, where $\lambda > 0$, $\Omega \in \mathbb{R}^{3\times3}$ is a matrix containing the intrinsic parameters depending on the sensor and lens characteristics, while $\Pi = [I_{3\times3},\, 0_{3\times1}] \in \mathbb{R}^{3\times4}$, with $I_{3\times3}$ being the identity matrix and $0_{3\times1}$ being the null vector. Assume to have two cameras (labeled as 1 and 2) with known intrinsic parameters, and refer to the triangulation method. It consists of computing the end-effector position $p = [p_x,\, p_y,\, p_z]^\top$ with respect to a base frame, starting from normalized coordinates in the image planes $\widetilde{s}_1 = [X_1, Y_1, 1]^\top$ and $\widetilde{s}_2 = [X_2, Y_2, 1]^\top$ of the projections of p, such that $\lambda_i\widetilde{s}_i = \Pi\widetilde{p}^i$, $i = 1, 2$, $\widetilde{p}^i$ being the coordinates with respect to the frame of the cameras. Assuming to have the vision base frame on camera 1, the following system can be written as

$$\begin{cases} \widetilde{p}^1 = \lambda_1\widetilde{s}_1 \\ \widetilde{p}^1 = o^1_{1,2} + \lambda_2 R^1_2 \widetilde{s}_2 \,, \end{cases} \tag{1}$$

where $o^1_{1,2}$ is the position vector of the frame of camera 2 with respect to the frame of camera 1, and R^1_2 is the corresponding rotation matrix. By solving system (1) with respect to $\widetilde{p}^1$, and considering the homogeneous transformation matrix T^b_1, finally, one has the position of the end-effector with respect to the base frame of the overall system assumed for instance on the first joint of the robot, i.e., $\widetilde{p} = T^\mathrm{b}_1\widetilde{p}^1$.

B. Orientation reconstruction

It is also necessary to find in real-time the orientation of the end-effector with respect to the base frame. This can be done by determining the homogeneous transformation matrix T^b_e. Assuming to acquire the vector of the projection of N points of the end-effector on the image plane of camera 1, the ith component of which is $s^{[i]}_1 = [X^{[i]}_1, Y^{[i]}_1]^\top$, then, by making a simple change of reference frame, the coordinates of these points can be written with respect to the reference frame of the camera itself as

$$\lambda_1\widetilde{s}^{[i]}_1 = \Pi T^1_\mathrm{e}\widetilde{p}^\mathrm{e}_{[i]}, \quad i = 1,\ldots,N \,. \tag{2}$$

This is a set of N equations from which it is possible to compute T^1_e. Then, solving system (2), the end-effector position and orientation with respect to the base frame results in being $T^\mathrm{b}_\mathrm{e} = T^\mathrm{b}_1 T^1_\mathrm{e}$. Hence, it is possible to obtain the robot joint variables q_v, by inverting the kinematics.

III. Problem Settings

In this section the considered robot model and type of faults are described, and the problem to solve is formulated.

A. Robot modelling

Consider a robotic system with n-joints. Let ℓ_i, $i = 1, 2, \ldots n$ denote the length of the ith link, let q_1 denote the orientation of the first link with respect to y-axis clockwise positive, and let q_j, $j = 2, 3, \ldots n$, denote the displacement of the jth link with respect to the $(j-1)$th one clockwise positive. Let $O(x, y, z)$ be the base-frame of the robotic manipulator, while $O_\mathrm{e}(n, s, a)$ be the end-effector frame.

1) Kinematics: The direct kinematics of a n-joints manipulator describes the relationship between the joint variables $q \in \mathbb{R}^n$ and the end-effector position and orientation in the workspace, according to the following expression

$$\begin{cases} p = p(q) \\ R^\mathrm{b}_\mathrm{e} = R^\mathrm{b}_\mathrm{e}(q) \end{cases} \tag{3}$$

where $p = [p_x,\, p_y,\, p_z]^\top$ is the position of the end-effector with respect to the base frame, and R^b_e is the rotation matrix between the reference frame attached to the end-effector and the base frame. In a more compact form, the direct kinematics can be expressed in terms of the following homogeneous transformation matrix

$$T^\mathrm{b}_\mathrm{e} = \begin{bmatrix} R^\mathrm{b}_\mathrm{e} & p \\ 0^\top_{1\times3} & 1 \end{bmatrix} . \tag{4}$$

2) Dynamics: The dynamics of the robot can be described in the joint space, by using the Lagrangian approach, as

$$B(q)\ddot{q} + n(q,\dot{q}) = \tau \tag{5}$$

$$n(q,\dot{q}) = C(q,\dot{q})\dot{q} + F_\mathrm{v}\dot{q} + F_\mathrm{s}\,\mathrm{sgn}(\dot{q}) + g(q) \tag{6}$$

TABLE I

Possible scenarios in case of Fault Events (FEs)

FEs	$\#_\mathrm{SF} = 1$	$\#_\mathrm{SF} > 1$	$\#_\mathrm{AF} = 1$	$\#_\mathrm{AF} > 1$
FE1			✓	
FE2	✓			
FE3				✓
FE4		✓		
FE5		✓		✓

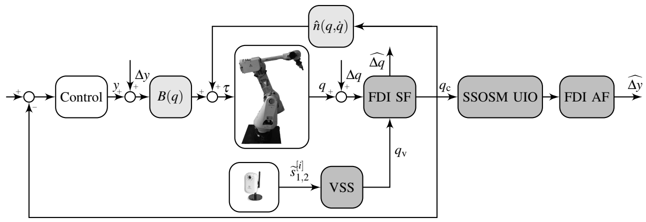

Fig. 1. The proposed fault diagnosis scheme for the considered COMAU SMART3-S2 robot manipulator with camera Atlantis NetCamera 500

where $B(q) \in \mathbb{R}^{n\times n}$ is the inertia matrix, $C(q,\dot{q}) \in \mathbb{R}^{n\times n}$ represents centripetal and Coriolis torques, $F_{\rm v} \in \mathbb{R}^{n\times n}$ is the viscous friction matrix, $F_{\rm s} \in \mathbb{R}^{n\times n}$ is the static friction matrix, $g(q) \in \mathbb{R}^{n}$ is the vector of gravitational torques and $\tau \in \mathbb{R}^{n}$ represents the motors torques.

B. Faults modelling

In this paper, the number (#) and type of fault events (FEs) which are taken into account are those indicated in Table I. For the sake of simplicity and in a quite realistic way, it is assumed that both sensor and actuator faults can be regarded as additive terms affecting the joint variable q and the torque vector τ, respectively.

Thus, let $\Delta\tau \in \mathbb{R}^{n}$ and $\Delta q \in \mathbb{R}^{n}$ denote the generic actuator fault (AF) and sensor fault (SF). In case of fault events on both these components of the plant, the control system receives $\bar{q} = q + \Delta q$ as angular displacements of the joints, while the actual torque applied to the robot can be expressed as $\bar{\tau} = \tau + \Delta\tau$. Hence, the dynamical model of the robot can be written as

$$B(\bar{q})\ddot{\bar{q}} + n(\bar{q},\dot{\bar{q}}) = \bar{\tau} \, . \quad (7)$$

IV. The Proposed Fault Diagnosis System

The proposed diagnosis scheme for robot manipulators is that illustrated in Figure 1. The key element is the so-called redundant sensor (in our case, it is a low cost IP camera). The use of this sensor can appear to be trivial, but it is actually the way to circumvent the difficulties in the detection of sensor and actuator faults which can occur at the same time. The redundant sensor allows one to detect and isolate faults on the sensors. In addition, the measurements it provides can be used, in case of sensor faults, to close the feedback, making the adopted control approach fault tolerant. More specifically, for the ith joint:

$$q_{{\rm c}_i}(t) = \begin{cases} q_{{\rm v}_i}(t) & \#_{\rm FEs} \neq 0 \\ q_i(t) & \text{otherwise} \end{cases} \quad (8)$$

where $q_{{\rm c}_i}$ is the ith component of vector $q_{\rm c}$ indicated in Figure 1, and $q_{\rm v}$ is the actual position of the robot provided by the IP camera. Since the feedback is closed using $q_{\rm c}$, one has that, independently of the presence of sensor faults, the so-called "inverse dynamics" control can be adopted to simplify the MIMO nonlinear robotic system. This is transformed into n perturbed double integrators, n being the number of degrees of mobility of the robot. The feedback linearization produced by the inverse dynamics control allows the designer to independently consider each joint, which is an advantage to perform the detection and isolation of the actuator faults.

A. Fault diagnosis logic for sensors

The vision block is assumed to provide the correct position of the joints with a sampling time which can be longer than that of the measurements provided by onboard sensors. For the sake of generality, assume that $\tau_{\rm v}$ is the vision-based data sampling time, and that $\tau_{\rm s}$ is the sensor (i.e., robot) sampling time. Then, the following hold mechanism is introduced

$$\begin{array}{ll} q_{{\rm v}_i}(t) = q_{{\rm v}_i}(k\tau_{\rm v}), & k\tau_{\rm v} \le t \le (k+1)\tau_{\rm v} \\ q_{{\rm s}_i}(t) = q_{{\rm s}_i}(k\tau_{\rm s}), & k\tau_{\rm s} \le t \le (k+1)\tau_{\rm s} \end{array} , \quad \forall k \ge 0 \, . \quad (9)$$

The position retrieved from the acquired images is compared with the actual robot position obtained from the sensors. The resulting signals represent the estimate of the displacement between the sensors output and the real position of the robot, called

$$\widehat{\Delta q}_i(t) = q_{{\rm s}_i}(t) - q_{{\rm v}_i}(t) \, . \quad (10)$$

Let $q_{{\rm s}_i}$ denote the measurement of the position of the ith joint obtained from the sensor, in order to detect the faults on the sensors the following flag function is defined

$$f_{{\rm s}_i} = \begin{cases} 0 & -\underline{Q}_{{\rm s}_i} < \widehat{\Delta q}_i(t) \le 0 \, \vee \, 0 < \widehat{\Delta q}_i(t) \le \overline{Q}_{{\rm s}_i} \\ 1 & \text{otherwise} \end{cases} \quad (11)$$

where $\underline{Q}_{{\rm s}_i}$ and $\overline{Q}_{{\rm s}_i}$ are positive numbers indicating the lower and the upper threshold values, respectively. Ideally, they should be equal to zero, but noise both on fastened sensors and in the vision system needs to be taken into account. If $f_{{\rm s}_i}$ returns 1 on the ith component, then a fault is detected on the corresponding sensor.

Apart from sensor FDI, the identification of the detected fault on the ith sensor can be also obtained by considering the time evolution of the difference signal (10).

B. Inverse dynamics

In this paper, in order to transform the nonlinear MIMO robotic system into a set of linear systems, the so-called inverse dynamics approach is used [15]. The inverse dynamics of the robot manipulator can be written, in the joint space, relying on (5)-(6), as a nonlinear relationship between the plant inputs and the plant outputs,

$$\tau = B(q_{\rm c})y + \hat{n}(q_{\rm c},\dot{q}_{\rm c}) \quad (12)$$

with $q_{\rm c}$ as in (8), y being an auxiliary control variable, $B(\cdot)$ coinciding with the actual one, while $\hat{n}(\cdot,\cdot)$ being an estimate of n. By applying the inverse dynamics control to system (5)-(6), one has

$$\begin{array}{l} \ddot{q}_{\rm c} = y - \eta(q_{\rm c},\dot{q}_{\rm c}) \\ \eta(q_{\rm c},\dot{q}_{\rm c}) = B^{-1}(q_{\rm c})(\hat{n}(q_{\rm c},\dot{q}_{\rm c}) - n(q_{\rm c},\dot{q}_{\rm c})) \end{array} \quad (13)$$

where $\eta(\cdot,\cdot)$ takes into account the modelling uncertainties and, possibly, external disturbances. Note that in this paper, as it is reasonable in field implementation, we assume that $\eta \in \mathcal{H}$

with $\mathcal{H}^{\sup} := \sup_{\eta\in\mathcal{H}}\{\|\eta\|\}$ known. Equation (13) shows how the original MIMO system is transformed into a set of n SISO decoupled systems subject to matched uncertainty. In case of fault on the actuators, substituting (12) in (7), it is possible to describe how the fault is mirrored on the auxiliary control variable, i.e., $\Delta y = -B^{-1}(q_{\rm c})\Delta\tau$ so that, the single joint dynamics results $\ddot{q}_{{\rm c}_i}(t) = y_i(t) + \Delta y_i(t) - \eta_i(t)$.

C. Sliding mode based observers for actuators

The fault diagnosis method for actuator faults proposed in this paper is based on the use of a SSOSM based Unknown Input Observer (UIO). In the considered case, it is assumed that the inverse dynamics control is applied. Then, it seems natural to design the observer relying on the model of the feedback linearized system. As such, the proposed UIO is the following

$$\ddot{\hat{q}}_{{\rm c}_i} = y_i(t) + u_i(t) \tag{14}$$

where $\hat{q}_{{\rm c}_i}$ is the observer state variable, y_i is the ith component of the auxiliary control variable, while u_i is the input of the observer. This signal is chosen according to the SSOSM approach [17]. Let $e_i \in \mathbb{R}^2$ be the estimation error, such that $e_{1_i} = q_{{\rm c}_i} - \hat{q}_{{\rm c}_i}$ and $e_{2_i} = \dot{q}_{{\rm c}_i} - \dot{\hat{q}}_{{\rm c}_i}$. Then, for any joint, a sliding variable is chosen as a linear combination of the estimation error and its first time derivative

$$\sigma_i = \beta_i e_{1_i} + e_{2_i} \tag{15}$$

where β_i is a positive constant. Assume $\xi_{1_i} = \sigma_i$ and $\xi_{2_i} = \dot{\sigma}_i$, then the so-called "auxiliary system" results in being

$$\begin{cases} \dot{\xi}_{1_i}(t) = \xi_{2_i}(t) \\ \dot{\xi}_{2_i}(t) = \beta_i \dot{e}_{2_i}(t) + \frac{d^{(3)}q_{{\rm c}_i}(t)}{dt^3} - \dot{y}_i(t) - w_i(t) \\ w_i(t) = \dot{u}_i(t) \ . \end{cases} \tag{16}$$

To be able to refer to the appreciable finite time convergence results related to the SSOSM approach it is required that the drift term in the second equation of (16) is bounded. Since the considered plant is a mechanically constrained robotic system, this assumption is surely satisfied. So, indicating with F_i the bound for joint i, one has

$$\left| \beta_i \dot{e}_{2,i}(t) + \frac{d^{(3)}q_{{\rm c}_i}(t)}{dt^3} - \dot{y}_i(t) \right| < F_i \ . \tag{17}$$

Finally, following the SSOSM design, the observer auxiliary control variable is chosen as

$$w_i(t) = \alpha_i W_{\max_i} \operatorname{sgn}\left(\xi_{1_i}(t) - \tfrac{1}{2}\xi_{\max_i}(t)\right) \tag{18}$$

with α_i and $W_{\max_i}$ being positive parameters to be suitably selected as follows

$$\alpha_i \in (0,\ 1] \cap (0,\ 3), \quad W_{\max_i} > \max\left(\frac{F_i}{\alpha_i}; \frac{4F_i}{3-\alpha_i}\right) \tag{19}$$

so as to enforce a second-order sliding mode on the sliding manifold $\sigma_i = 0$, and $\xi_{\max_i}$ being the last extremal value of the sliding variable, i.e., the last value of ξ_{1_i}(t) in correspondence of which ξ_{2_i} is equal to zero. Note that, the observer input is continuous, since it is the output of an integrator.

Now, it is convenient to make reference to the concept of "equivalent control" (see [26] for a definition in case of relative degree one systems subject to a discontinuous control input). This concept has been extended to systems exhibiting second-order sliding modes in [27]. By definition, the equivalent control (its ith component in the multi input case) is the continuous time control which solves the equation $\dot{\sigma}_i = 0$. Let $u_{{\rm eq}_i}$ be the ith equivalent control component in our case. It can be used as a residual to perform the FDI, according to the following rule

$$f_{{\rm a}_i} = \begin{cases} 0 & -\underline{Q}_{{\rm a}_i} < u_{{\rm eq}_i} \le 0 \quad \text{or} \quad 0 < u_{{\rm eq}_i} \le \overline{Q}_{{\rm a}_i} \\ 1 & \text{otherwise} \end{cases} \tag{20}$$

where $\underline{Q}_{{\rm a}_i}$ and $\overline{Q}_{{\rm a}_i}$ are the activation thresholds, determined according to the known bounds of the uncertainty contributions.

D. Analysis of the fault diagnosis strategy

By applying the inverse dynamics control in (12), any single joint can be regarded as a linear decoupled second order system. Then the FDI rules (11) and (20) can be applied to each joint. Thanks to the use of vision, sensor faults can be detected, isolated and identified. It remains to prove that the equivalent signals $u_{{\rm eq}_i}$, $i = 1, \ldots, n$, are actually estimates of the actuator faults. To this end, the following result holds.

Theorem 1: Given the nonlinear coupled robotic model (5) and (6), applying the inverse dynamics control in (12), and the fault detection and isolation strategy in (11) and (20), considering the SSOSM UIO in (14)-(18), then any component i of the observer input law provides, after a transient time $t_{\rm r}$, an estimate $\widehat{\Delta y_i}$ of the ith fault, with an associated estimation error $\widetilde{\Delta y_i} = \Delta y_i - \widehat{\Delta y_i}$ such that $|\widetilde{\Delta y_i}| < \mathcal{H}^{\sup}$. □

Proof: The proof of convergence directly follows from [17], while the computation of the estimation error and its bound are derived from the equivalent control signal $u_{{\rm eq}_i}$. ■

According to [26], a practical way to retrieve the equivalent control signal $u_{{\rm eq}_i}$ is to filter the discontinuous control input via a low-pass filter. In the present case it can be found at the output of the integrator indicated in (16).

V. Case Study

In this section simulation and experimental results are reported to complement the theoretical discussion.

TABLE II
SCENARIO FE5

$\#_{\rm joint}$	FE	$t_{\rm o}$ [s]	$\Delta*(t)$ $(* \doteq q, y)$
1	AF	9	30 $[{\rm rad\,s^{-2}}]$
	SF	8	$0.3\sin(2t)$ [rad]
2	AF	9	$40\sin(t)$ $[{\rm rad\,s^{-2}}]$
	SF	–	–
3	AF	11	-60 $[{\rm rad\,s^{-2}}]$
	SF	–	–

TABLE III

SIMULATION PARAMETERS

$\#_{\text{joint}}$	$\underline{Q}_{s_i}$	$\overline{Q}_{s_i}$	$\underline{Q}_{a_i}$	$\overline{Q}_{a_i}$	β_i	α_i	$W_{\max_i}$
1	0.02	0.02	3	3	10	0.9	30000
2	0.05	0.05	11	5	10	0.9	60000
3	0.04	0.02	8	65	10	0.9	100000

TABLE IV

EXPERIMENTAL PARAMETERS

$\#_{\text{joint}}$	$\underline{Q}_{s_i}$	$\overline{Q}_{s_i}$	$\underline{Q}_{a_i}$	$\overline{Q}_{a_i}$	β_i	α_i	$W_{\max_i}$
1	0.02	0.02	3	3	10	0.9	40000
2	0.05	0.05	11	5	10	0.9	150000
3	0.03	0.03	8	65	10	0.9	400000

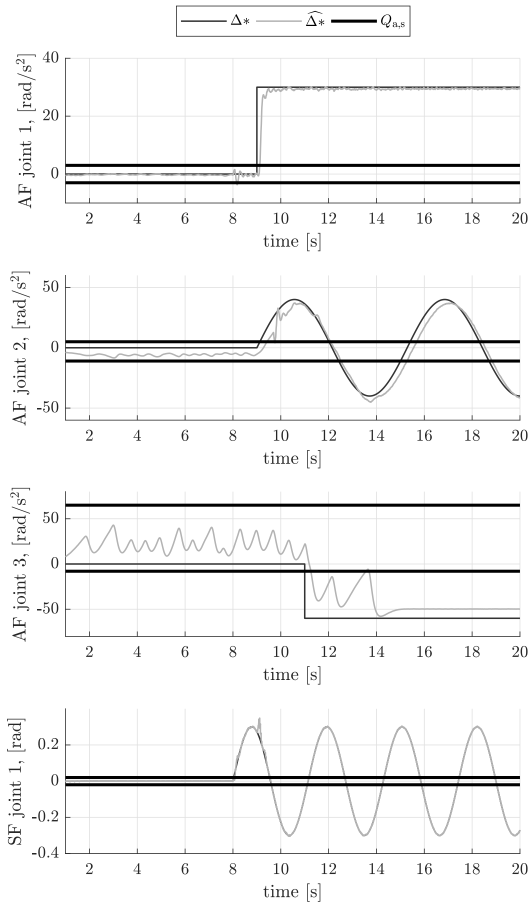

Fig. 2. Simulation results: multiple faults both on actuators 1, 2 and 3, and on sensor 1

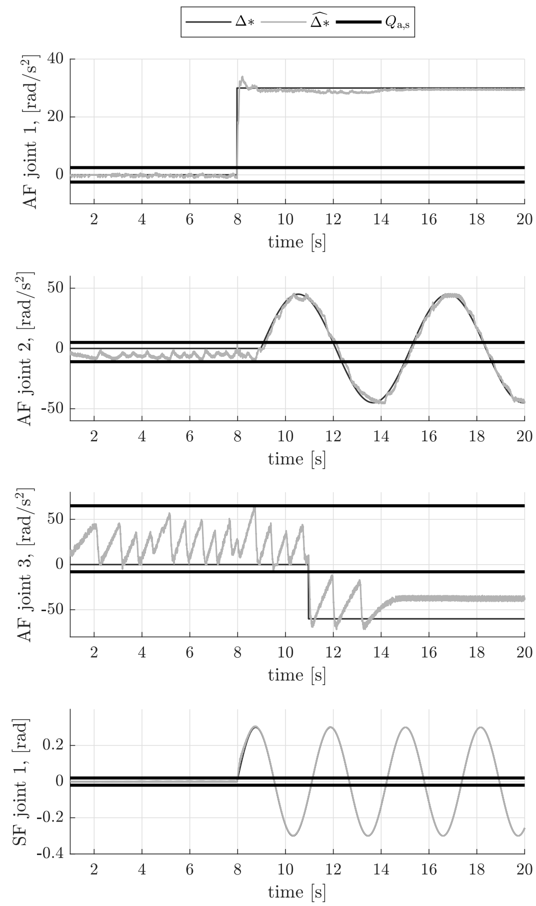

Fig. 3. Experimental results: multiple faults both on actuators 1, 2 and 3, and on sensor 1

A. Experimental setup

The verification and validation of the concept underlying the proposal of this paper have been performed in simulation and experimentally with reference to a COMAU SMART3-S2 industrial anthropomorphic robot manipulator. For the sake of simplicity, only three joints are used in the testing phase, so that the model of the robot identified as in [21] can be adopted for simulation, and a single camera can be used as vision sensor. This latter is, in our lab set-up, a low-cost IP camera of type Atlantis NetCamera 500. The Round Trip Time (RTT) of the camera is approximately 30 ms.

To assess the effectiveness of the proposed fault diagnosis strategy, we have considered the injected faults reported in Table II, where the AFs are expressed in terms of corresponding acceleration. They occur both on the actuators and on the sensors (scenario FE5 in Table I), and their occurrence time is t_{o}.

B. Simulation results

In this subsection we assess the performance of the proposed fault diagnosis strategy in simulation, relying on the model of the considered robot manipulator. In order to better emulate the real robot, the noise term $\eta = [\eta_1, \eta_2, \eta_3]^\top$, experimentally acquired, is injected to the accelerations of the joints. The noise term components are bounded with bounds which can be determined by signal processing methods during the experimental tests, i.e., $-2.3 \leq \eta_1 \leq 2.1$, $-10.3 \leq \eta_2 \leq 0.3$, $-6.9 \leq \eta_3 \leq 59.2$.

Since the sliding mode-based observers prove to converge in a finite time t_{r}, we have considered a time instant $t_{\text{c}} \geq t_{\text{r}}$, from which the observed variables in (14) become usable, since the observer transient phase has elapsed. Moreover, the IP camera is simulated assuming that it is a block which provides the correct value of the joint angles with a sampling time, as in the real case, of 30 ms. To perform the simulation tests, the Euler solver is used with a numerical integration step equal to 0.001 s. Table III reports the thresholds used by FDI logic both for the actuators and for the sensors and the parameters of the SSOSM UIO used for each joint. Note that, in order to better identify the shape of the faults, a low pass filter with a time constant of 0.1 s is applied to the detected signals. Figure 2 shows the behavior of the proposed strategy. All the faults have been correctly detected, isolated and identified.

C. Experimental results

The proposed control approach has also been experimentally verified by performing tests on the actual COMAU SMART3-S2 industrial anthropomorphic robot manipulator. The parameters used in the experimental tests are reported in Table IV. Note that the parameters used in simulation have been regarded as a starting choice to perform the tuning of the parameters used in the experimental tests. Also in this case, a low pass filter is applied to the detected signals to improve the fault identification. Figure 3 shows the effectiveness of the proposed strategy in the same scenario considered in simulation. In all cases, the simulation results are confirmed also experimentally.

VI. Conclusions

In this paper, a fault detection, isolation and identification scheme for robot manipulators has been presented. The proposed approach is based on the joint application of an inverse dynamics-based feedback linearizing control and of a fault detection and isolation logic. The use of an IP camera, which is a low cost vision sensor in our case, allows one to attain a complete sensor fault diagnosis, apart from providing estimates of the controlled variables which can be used to close the control feedback in case of faulty behavior, making the robot control system tolerant to sensor faults. The additional use of n SSOSM UIOs also enables the actuator fault diagnosis with appreciable robustness features. Future work will be devoted to the analysis of the vision system and its impact on the proposed fault diagnosis method.

VII. Acknowledgments

The authors gratefully acknowledge the contribution and the full help provided by the senior lab technician Gianluca De Felici and by the master student Diego Franzosi during the experimental tests.

References

[1] R. Isermann, *Fault-Diagnosis Systems: An Introduction from Fault Detection to Fault Tolerance*. Springer, 2006.

[2] H. Natke and C. Cempel, *Model-Aided Diagnosis of Mechanical Systems: Fundamentals, Detection, Localization, Assessment*. Springer London, 2011.

[3] L. Chiang, R. Braatz, and E. Russell, *Fault Detection and Diagnosis in Industrial Systems*, ser. Advanced Textbooks in Control and Signal Processing. Springer London, 2001.

[4] M. Simandl and I. Puncochar, "Active fault detection and control: Unified formulation and optimal design," *Automatica*, vol. 45, no. 9, pp. 2052–2059, 2009.

[5] A. Esna Ashari, R. Nikoukhah, and S. Campbell, "Active robust fault detection in closed-loop systems: Quadratic optimization approach," *IEEE Transactions on Automatic Control*, vol. 57, no. 10, pp. 2532–2544, 2012.

[6] J. K. Scott, R. Findeisen, R. D. Braatz, and D. M. Raimondo, "Input design for guaranteed fault diagnosis using zonotopes," *Automatica*, vol. 50, no. 6, pp. 1580–1589, 2014.

[7] V. Venkatasubramanian, R. Rengaswamy, K. Yin, and S. N. Kavuri, "A review of process fault detection and diagnosis: Part i: Quantitative model-based methods," *Computers and Chemical Engineering*, vol. 27, no. 3, pp. 293–311, 2003.

[8] B. Halder, *Robust Nonlinear Fault Detection and Isolation of Robotic System: A novel nonlinear analytic redundancy method*. VDM Verlag, 2009.

[9] G. G. Rigatos, *Fault Diagnosis in Robotic and Industrial Systems*, 1st ed. iConcept Press Ltd., 2012.

[10] A. De Luca and R. Mattone, "An adapt-and-detect actuator FDI scheme for robot manipulators," in *Proceedings International Conference on Robotics and Automation*, vol. 5, Barcelona, Spain, Apr. 2004, pp. 4975–4980.

[11] ——, "An identification scheme for robot actuator faults," in *Proceedings IEEE/RSJ International Conference on Intelligent Robots and Systems*, Alberta, Canada, Aug. 2005, pp. 1127–1131.

[12] A. Papadimitropoulos, G. A. Rovithakis, and T. Parisini, "Fault detection in mechanical systems with friction phenomena: An online neural approximation approach," *IEEE Transactions on Neural Networks and Learning Systems*, vol. 18, no. 4, pp. 1067–1082, 2007.

[13] L. M. Capisani, A. Ferrara, A. Ferreira de Loza, and L. M. Fridman, "Manipulator fault diagnosis via higher order sliding-mode observers," *IEEE Transactions on Industrial Electronics*, vol. 59, no. 10, pp. 3979–3986, 2012.

[14] L. M. Capisani, A. Ferrara, and P. Pisu, "Sliding mode observers for vision-based fault detection, isolation and identification in robot manipulators," in *Proceedings American Control Conference*, Baltimore, Maryland, USA, Jun. 2010, pp. 4540–4545.

[15] B. Siciliano, L. Sciavicco, L. Villani, and G. Oriolo, *Robotics-Modelling, Planning and Control*, 3rd ed. London, UK: Springer-Verlag, 2009.

[16] G. Bartolini, A. Ferrara, A. Levant, and E. Usai, *On second order sliding mode controllers*, ser. Lecture Notes in Control and Information. London, UK: Springer-Verlag, 1999, pp. 329–350.

[17] G. Bartolini, A. Ferrara, and E. Usai, "Chattering avoidance by second-order sliding mode control," *IEEE Transactions on Automatic Control*, vol. 43, no. 2, pp. 241–246, Feb. 1998.

[18] L. M. Capisani, A. Ferrara, and L. Magnani, "Design and experimental validation of a second-order sliding-mode motion controller for robot manipulators," *Interantional Journal of Control*, vol. 82, no. 2, pp. 365–377, Jan. 2009.

[19] G. P. Incremona, A. Saccon, A. Ferrara, and H. Nijmeijer, "Trajectory tracking of mechanical systems with unilateral constraints: Experimental results of a recently introduced hybrid pd feedback controller," in *Proceedings 54th IEEE Conference on Decision and Control*, Osaka, Japan, Dec. 2015, pp. 920–925.

[20] A. Ferrara and G. P. Incremona, "Design of an integral suboptimal second-order sliding mode controller for the robust motion control of robot manipulators," *IEEE Transactions on Control Systems Technology*, vol. 23, no. 6, pp. 2316–2325, Nov. 2015.

[21] G. P. Incremona, A. Ferrara, and L. Magni, "MPC for robot manipulators with integral sliding modes generation," *IEEE/ASME Transactions on Mechatronics*, vol. 22, no. 3, pp. 1299–1307, 2017.

[22] J. Davila, L. Fridman, and A. Poznyak, "Observation and identification of mechanical systems via second order sliding modes," *International Journal of Control*, vol. 79, no. 10, pp. 1251–1262, 2006.

[23] S. K. Spurgeon, "Sliding mode observers: a survey," *International Journal of Systems Science*, vol. 39, no. 8, pp. 751–764, 2008.

[24] H. Alwi, C. Edwards, and C. P. Tan, *Fault Detection and Fault-Tolerant Control Using Sliding Modes*, ser. Advances in Industrial Control. Springer, 2011.

[25] D. Brambilla, L. Capisani, A. Ferrara, and P. Pisu, "Fault detection for robot manipulators via second-order sliding modes," *IEEE Transactions on Industrial Electronics*, vol. 55, no. 11, pp. 3954–3963, 2008.

[26] V. I. Utkin, *Sliding Modes in Optimization and Control Problems*. New York: Springer Verlag, 1992.

[27] G. Bartolini, A. Ferrara, and E. Usai, "On boundary layer dimension reduction in sliding mode control of siso uncertain nonlinear systems," in *Proceedings IEEE International Conference on Control Applications*, vol. 1, Trieste, Italy, Sep. 1998, pp. 242–247.